Journal of Structural Geology, Vol. 14, No. 8/9, pp. 1007 to 1017, 1992
Printed in Great Britain

0191-8141/92 $05.00+0.00

Regional state of stress, fault kinematics and adjustments of blocks in a fractured body of rock: application to the microseismicity of the Rhine graben

E. CAREY-GAILHARDIS and J. L. MERCIER

URA (CNRS 1369) Laboratoire de Géophysique et Géodynamique interne, Bât. 509, Université de Paris Sud, 91405 Orsay Cédex, France

(*Received* 1 *November* 1991; *accepted in revised form* 9 *April* 1992)

Abstract—A simple mechanical model of a homogeneous state of stress and independent fault motions is generally used to interpret fault kinematics in terms of stress. However analysis of focal mechanisms of microearthquakes shows that, as a result of incompatibilities of block motions in an assemblage of rigid or elastic blocks, deformation of a fractured body of rocks is in general heterogeneous. Analyses of focal mechanism sets show that they are in general composed of a main group whose fault motions result from a mean state of stress (TM) in good agreement with the regional state of stress; the remaining complex fault motions are explained by a compressional (TC) and/or a tensional deviator (TE). An important observation is that within the computed uncertainties, these (TC) and (TE) deviators are co-axial with the mean state of stress (TM). These deviators statistically model the local fault-slips probably due to the incompatibilities of block motions and cannot be considered as other mean states of stress. Thus if the regional state of stress is known for a fault plane whose strike and dip are given, its kinematics cannot be surely predicted. Two types (TC and TE) of motions different from that (TM) predicted by the regional state of stress may exist; they are the kinematic instabilities. As a consequence all the motions shown by focal mechanisms or by striated faults are not significant of the regional tectonic regime. This is well illustrated by the microseismicity of the Rhine graben where it is shown that the compressional fault motions are kinematic instabilities, and the extensional fault motions are representative of a regional state of stress (σ_1 vertical) with a N45°-trending σ_3 axis. Hence, the simple mechanical model of homogeneous state of stress and independant fault motions is valid only if there are no incompatibilities of block motions. Possibly, these incompatibilities may be accommodated by a pressure-solution–crystallization process for creep faulting or by internal cataclastic deformation of large blocks separated by major stick–slip faults.

INTRODUCTION

FOCAL solutions of shallow earthquakes ($\mathbf{M} \geq 6$) which have affected a region are often coherent with respect to a regional direction of compression and/or of extension. This suggests that kinematics of large superficial seismic faults are controlled by a mean regional state of stress. Inference of this state of stress is a problem similar to that concerning striated fault plane populations (e.g Carey & Brunier 1974, Armijo & Cisternas 1978, Angelier & Goguel 1979, Etchecopar *et al.* 1981). It is now current practice to interpret these focal mechanisms in terms of stress using a simple mechanical model of homogeneous state of stress and inversion techniques. But aftershock sequences of large earthquakes or microseismic activity ($\mathbf{M}_L \leq 4$) show very complex focal mechanism populations (Hatzfeld *et al.* 1987) indicating that kinematics of minor seismic faults cannot result from an homogeneous state of stress. Some motions are in agreement with the mean regional state of stress, deduced in the same area for example by analysis of recent Quaternary faults; others are not. This suggests the occurrence of characteristic fault kinematic instabilities in a fractured body of rock submitted to a regional state of stress. Fortunately, such complex focal mechanism populations can be modelled in a simple manner (Mercier & Carey-Gailhardis 1989) and this may lead to the determination of a mean stress deviator which is in good agreement with the regional state of stress. In this paper we briefly recall the methodology for analysing focal mechanisms of major earthquakes and microearthquakes in terms of stress. We then suggest a qualitative model for explaining the occurrence of fault kinematic instabilities, and as an example we show that in the Rhine graben and surrounding regions all the focal solutions of the microearthquakes are not indicative of the regional tectonic regime.

METHODOLOGY FOR ANALYSING FOCAL MECHANISMS OF MAJOR EARTHQUAKES IN TERMS OF STRESS

To model kinematics of seismic faults shown by focal mechanisms of major earthquakes ($\mathbf{M} \geq 6$) we use a simple model (Carey & Brunier 1974) which supposes the following hypotheses. (1) The analysed body of rock is physically homogeneous and isotropic and, if prefractured, is also mechanically isotropic, i.e the orientation of the fault planes is random. (2) Displacements on the fault planes are small with respect to their lengths and there is no ductile deformation of the material and thus no rotations of the fault planes. Moreover the computation assumes that (3) a tectonic event is characterized by a single homogeneous stress tensor, (4) the slip responsible for the striation occurs on each fault plane in the direction and the sense of the resolved shear stress acting on the fault plane, and (5) the slips on the fault planes are independent of each other.

The orientation of the resolved shear stress τ_i on a fault plane is a function of four parameters defining the orientation of the principal stress axes, and the stress ratio R which is based on the differences of the principal deviatoric stress values (Bott 1959) such that $R = (\sigma'_2 - \sigma'_1)/(\sigma'_3 - \sigma'_1)$ $(0 < R < 1)$. Conversely the orientation of the slip-vectors $\mathbf{s}_i$ measured on a family of fault planes can lead to the computation of these parameters by minimizing the deviation between the predicted τ_i and the observed $\mathbf{s}_i$ slip-vectors on each fault plane (see Carey & Brunier 1974). Therefore, computation of states of stress from populations of focal mechanisms of earthquakes requires the knowledge of the seismic slip-vectors and consequently the selection of the preferred seismic fault plane from each couple of nodal planes. This can be obtained from the observation of the co-seismic activated fault plane on the ground, or by the spatial distribution of the aftershocks of large earthquakes. This selection is also possible by computation because only one of the two slip-vectors of a focal solution is the seismic slip-vector in agreement with the principal stress axes. For this slip-vector the ratio R, computed by Bott's (1959) formula (given above) is such that $0 < R < 1$. Moreover if one of the two nodal planes satisfies this condition, the other does not, except if the two nodal planes intersect each other along a principal stress axis. Several algorithms (Vasseur *et al.* 1983, Gephart & Forsyth 1984, Julien & Cornet 1987, Carey-Gailhardis & Mercier 1987, Rivera & Cisternas 1987) permit one to compute a stress deviator from a population of focal mechanisms of earthquakes which have occurred in the same area assuming a mean state of stress in the source region. In general the state of stress computed from teleseismic recordings is in good agreement with the state of stress deduced from recent and active faulting observed in the field and thus may be considered as a good evaluation of the regional state of stress. This is well illustrated, for example, by the seismicity of Tibet (Carey-Gailhardis & Mercier 1987).

Thus, in general, if the regional state of stress is known, the kinematics of a major fault plane whose strike and dip is given, may be computed and thus predicted within some uncertainties. Therefore at the scale of a body of rock cut by faults several kilometres long, deformation may be considered as homogeneous and the slips on the fault planes may be considered as independent of each other at a first approximation.

COMPUTATION OF THE STATE OF STRESS FROM FOCAL MECHANISMS OF MICROEARTHQUAKES

In contrast, focal mechanisms of microearthquakes, as for example those of the epicentral area of the 1978 Thessaloniki earthquake (northern Greece), often show complex fault kinematics (Hatzfeld *et al.* 1987) which cannot be modelled by a single stress deviator. This can be simply demonstrated. The σ_1 axis is located everywhere in the compressional right dihedra separated by the nodal planes which contains the P axis (McKenzie 1969) (conversely σ_3 is located everywhere in the tensional right dihedra). Therefore the necessary condition to compute a unique stress deviator which models a population of focal solutions is that the σ_1 axis is located in the common compressional area resulting from superimposition of all the focal mechanisms, likewise σ_3 is located in the common extensional area. Clearly the focal solutions of the microearthquakes of the Thessaloniki epicentral area do not satisfy this necessary condition (Fig. 1a) and cannot be modelled by a single stress deviator. Combining all the data of the focal mechanism set in groups of four data, a maximum of $n(n-1)(n-2)(n-3)/4!$ deviators can be computed; this is not a realistic solution. The simple, non-reducible solution separates two groups of focal mechanisms each of which satisfies the above necessary condition and leads to the computation of a stress deviator (Figs. 1b & c). One (TM) is extensional and is in good agreement with the regional state of stress in the northern Aegean (Mercier & Carey-Gailhardis 1989); the other (TC) is compressional and models reverse fault motions which are not in agreement with the regional tectonic regime. Separation of these two groups is obtained by a method of trial and error explained in Mercier & Carey-Gailhardis (1989). It has been obtained by a generalized inversion method (Carey-Gailhardis & Sotin 1991) which extracts the seismic fault planes and computes the stress deviator. The determination of the seismic fault planes is possible because the probability distribution of the characteristic parameters of these planes has a smaller standard deviation than that of the auxiliary planes. This generalized inversion method leads to the same deviators (see Table 3) and to the same choice of the preferred seismic fault planes as the previous method.

More complex focal mechanism sets such as that of the aftershock sequence of the 1980 Campania–Lucania earthquake (Deschamps & King 1984) may lead to the computation of three deviators (Mercier & Carey-Gailhardis 1989). One (TM) agrees with the regional extensional tectonic regime; the two other compressional (TC) and extensional (TE) deviators do not. We have also analysed the aftershock sequences of the 1971 San Fernando, California (Gephart & Forsyth 1984) and 1980 El Asnam, Algeria (Vasseur *et al.* 1983) earthquakes which occurred in regional compressional tectonic regimes. This leads to similar results. Compressional deviators (TM) in agreement with the regional tectonic regimes explain the reverse fault motions; other fault motions have a normal component and are modelled by an extensional deviator (TE).

Thus, in general, numerical analyses of focal mechanism populations of microearthquakes show (Mercier & Carey-Gailhardis 1989) (1) a main group whose fault motions result from a mean state of stress (TM) in agreement with the regional state of stress and (2) the remaining complex fault motions are explained by a compressional (TC) and/or a tensional (TE) stress deviator. An important observation is that, for each

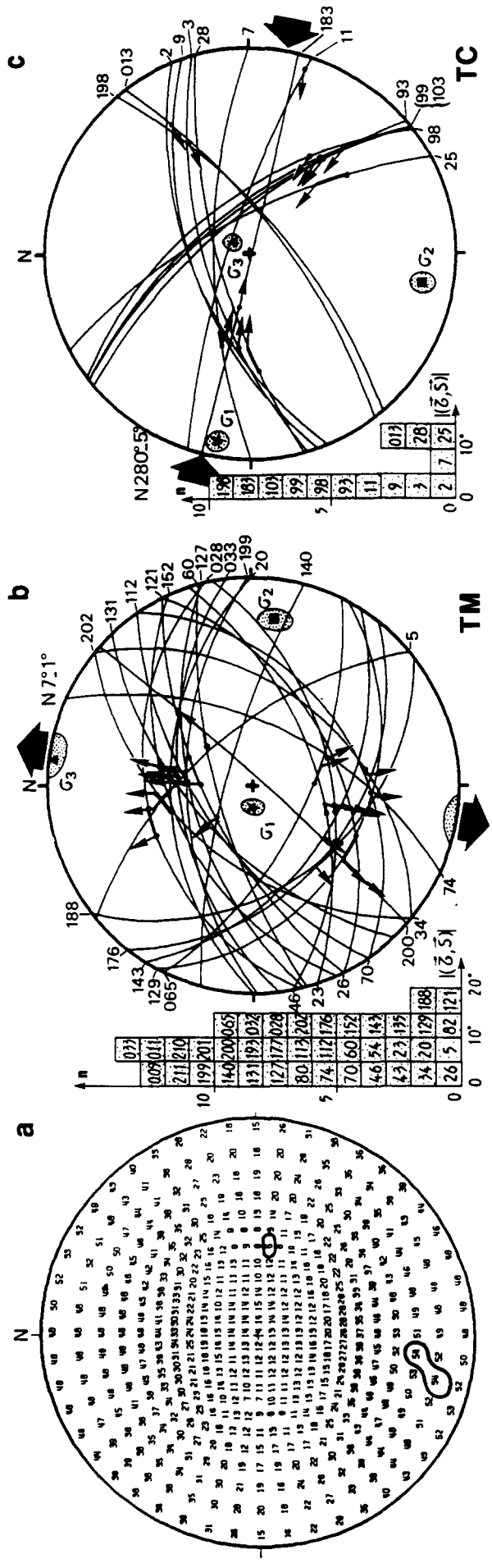

Fig. 1. Preferred seismic fault planes deduced from the focal mechanisms of the aftershock sequence of the 1978 Thessaloniki earthquakes. (a) Superimposition of the right dihedra limited by the nodal planes for the 55 studied focal mechanisms. The surrounded area shows the common extensional (highest numbers) and compressional (lowest numbers) zones; six data are outside the common compressional zone and the extensional common zone concerns 54 data. (b) & (c) Optimum stress models corresponding, respectively, to the mean state of stress (TM) and to the deviator (TC) which models the compressional local fault motions. The stippled areas show the zones surrounding the optimal stress axes which contain the stress axes of all the possible deviators giving a deviation (τ,s) smaller than 20° on each fault plane of the data set. Arrows on the great circles directed outward (resp. inward) the stereonet show normal (resp. reverse) fault motions. Histograms and thick lines on the great circles give the deviations (τ,s). Wulff projection, lower hemisphere. Numbers outside the stereonet and inside the histogram refer to the numbers of the data in Hatzfeld *et al.* (1987).

analysed example, these deviators are co-axial within the computed uncertainties (Figs. 1b & c).

This shows that, even if the regional state of stress is known, the kinematics of a minor fault plane whose strike and dip are given cannot be surely predicted. Several motions (TC, TE) different from that (TM) predicted by the regional state of stress may exist; these TC and TE motions are the kinematic instabilities. At the scale of a body of rock cut by faults some 100 m long or less, deformation must be considered as heterogeneous and slips on the fault planes are not independent.

HOW TO EXPLAIN THE FAULT KINEMATIC INSTABILITIES?

In a previous paper (Mercier & Carey-Gailhardis 1989) we analysed the numerical relations between the mean state of stress (TM) and the deviators (TC) and (TE) which model the different families of fault kinematic instabilities. Here, we simply propose a qualitative model to account for the occurrence of these instabilities (Mercier *et al.* 1991). This basically supposes that due to the incompatabilities of block motions, deformation at every point of the fractured body of rock is not homogeneous with the bulk deformation of this body. We suggest that in a fractured body of rock submitted to a regional state of stress, slips occur preferentially on pre-existing faults well-oriented with respect to the principal stress directions. Then if these faults are sufficiently numerous, block displacements statistically produce a bulk deformation of the block assemblage corresponding to a mean state of stress (TM). But incompatibilities of block motions exist and locally they produce internal elastic stresses in these blocks. These stresses must be relaxed by slips on the block boundaries or by formation of new fractures. As these local block motions are constrained by the neighbouring blocks, we suggest that they must be statistically compatible with the bulk deformation of the block assemblage. In this case, these local fault motions have to be statistically modelled by stress deviators (TE,TC) co-axial with the mean state of stress (TM) but having different orientations of the principal stress axes. These (TC) and (TE) deviators statistically model local slips on fault planes scattered in the block assemblage; therefore, they cannot be considered as other states of stress. For a given tectonic regime, the occurrence of the local fault motions, compressional (TC) or extensional (TE), probably depends on the stress ratio R: i.e on the compressional or tensional deviatoric value of the σ'_2 axis with respect to the σ'_1 value in a compressional tectonic regime and to the σ'_3 value in an extensional regime. It probably also depends on the geometry of the fracture net (Segall & Pollard 1980, Pollard & Saltzer 1991).

Thus, the kinematics of minor seismic faults indicate that deformation of an assemblage of rigid or elastic blocks is necessarily heterogeneous and that in such a medium, motions on faults cannot be modelled by a single stress tensor. Indeed, analyses of minor fault kinematics in the field sometimes lead to the computation of several coaxial deviators with different orientations of the principal stress axes, although structural data do not indicate a chronological succession of several sets of striations resulting from successive tectonic events (see Cabrera *et al.* 1991). Therefore, we think that these so-called 'permutations of the principal stress values' ($\sigma_2 \rightarrow \sigma_1$, $\sigma_1 \rightarrow \sigma_3$, Fig. 1) are not significant of temporal changes in the regional state of stress and may simply result from a heterogeneous deformation. They may be confused with real permutations of the principal stress values corresponding to spatial or temporal changes in the regional state of stress (see Mercier *et al.* 1991) in response to changes in the magnitude of the boundary or of the body forces.

Yet, it is often observed that a population of striated minor faults resulting from a single tectonic event leads to the computation of a single stress deviator. Indeed, striations measured in the field are often growth fibres and stylolitic striations which indicate creep fault motions. In such a case if a pressure-solution–crystallization process is active, it may accommodate the incompatibilities of block motions which should have occurred as a result of stick–slip faulting. Then, no local adjustments of blocks are necessary; deformation may be considered as homogeneous and the computed state of stress is the quasi-static state of stress.

Focal mechanisms of large earthquakes show that major seismic (i.e stick–slip) faults may also lead to the computation of a single stress deviator. In this case, blocks separated by the seismic faults are several kilometres in length and probably the incompatibilities of motions of these large blocks are accommodated by a cataclastic internal deformation (Jackson & McKenzie 1983). This suggests that the states of stress deduced from the analysis of minor faults reflect the internal deformation of the blocks separated by the major faults rather than the regional state of stress. Moreover, stress perturbations may occur as a result of mechanical interactions between neighbouring faults (Segall & Pollard 1980, Mattauer *et al.* 1991). Thus, only the coherence of the results shown for example by a statistical analysis of the principal stress directions obtained at numerous sites (see Mercier *et al.* 1991) may be a convincing argument for a reliable information on the regional principal stress directions.

ACTIVE TECTONICS IN THE RHINE GRABEN AND SURROUNDING REGIONS DEDUCED FROM THE MICROSEISMIC ACTIVITY: AN ALTERNATIVE VIEW

The maximum horizontal stress direction ($\sigma_{H\ max}$) in the Rhine graben and surrounding regions is well defined by numerous *in situ* stress measurements (Baumann & Illies 1983); it strikes N145.3° ± 14.2°. The mean P axis deduced from focal mechanisms of small earthquakes is in agreement with the above $\sigma_{H\ max}$

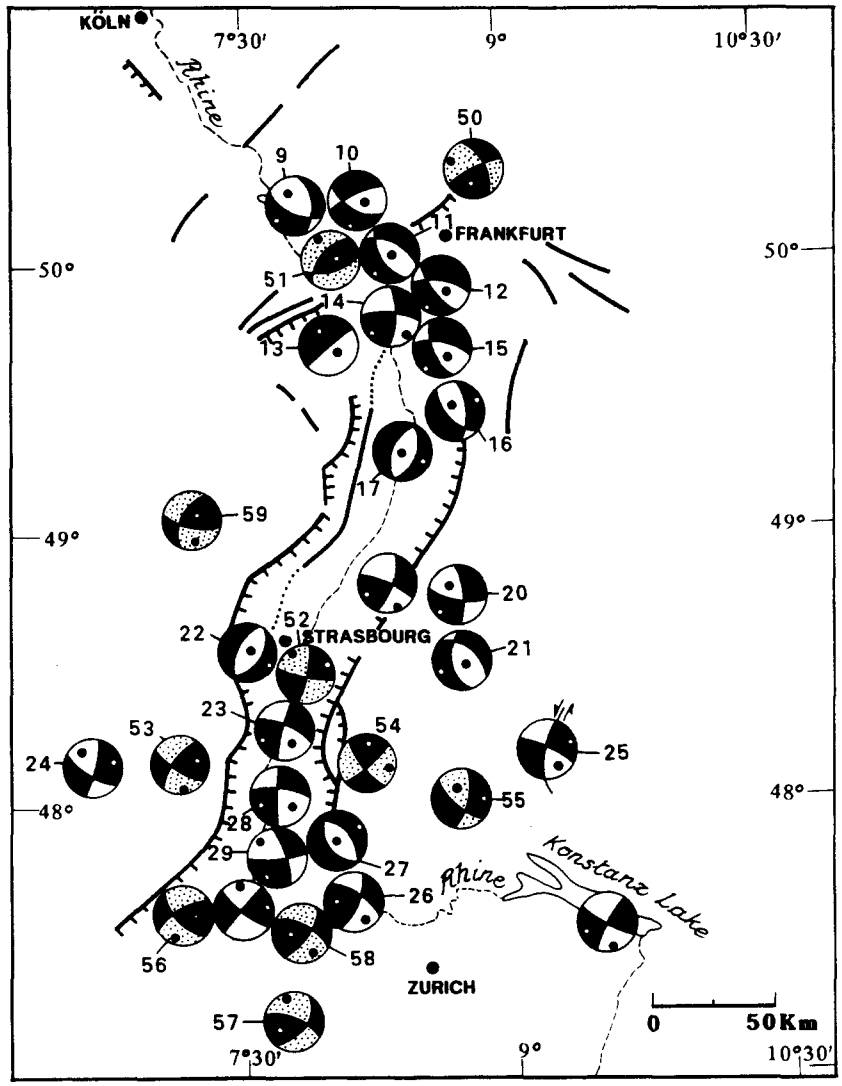

Fig. 2. Fault plane solutions (Wulf projection, lower-hemisphere) of the earthquakes in the Rhine graben area from 1971 to 1980 (after Bonjer *et al.* 1984, Larroque *et al.* 1987) used to compute the stress deviators FIC2 and FIC3 (Table 3). The black quadrants contain the T axes, and the P axes are located in the white quadrants for extensional focal mechanisms and in the dotted quadrants for compressional focal mechanisms. Numbers of the events are those of Tables 1 and 2.

direction; it trends N135° in the Rhenish Massif (Ahorner *et al.* 1983), N140° in the Rhine graben (Bonjer *et al.* 1984) and NNW–SSE in northern Switzerland (Pavoni 1987). The respective values of the vertical and horizontal stress axes are not generally known. In the northern part of the graben *in situ* stress measurements by hydrofracturing in the Soultz-sous-Forêt borehole (Rummel & Hansen 1988) have indicated a tensional state of stress (σ_1 vertical). In the southern part of the graben, in the potash mines of the Wittelheim region, *in situ* stress measurements by using hydrofractures show a variation of the stress magnitude according to the nature of the rocks. It indicates a strike-slip (σ_2 vertical) or a normal (σ_1 vertical) faulting regime (Cornet & Burlet in press). Structural analysis of faults in the Rhine graben region demonstrates horizontal σ_1 and σ_3 axes trending N130°–150° and N40°–60°, respectively (Bergerat 1985, Villemin & Bergerat 1985). This strike-slip faulting regime is believed to be of Pliocene–Quaternary age but it is not accurately dated other than being post-Oligocene. Inversion of focal mechanisms of microearthquakes (Larroque *et al.* 1987) suggests an extensional tectonic regime in the northern part of the Rhine graben, but a strike-slip regime in the southern part. This latter tectonic regime is deduced from the occurrence of compressional focal solutions in the analysed focal mechanism set (Fig. 2). However, some compressional focal mechanisms are also observed in the northern part of the graben and in the Rhenish Massif, although there the tectonic regime is considered to be clearly extensional. Thus it may be wondered if these compressional focal solutions in the northern as well as the southern part of the graben do not simply reverse fault motions resulting from adjustments of blocks and if they are really significant of the regional state of stress.

Computation of the stress deviators from the microseismic activity

Following the methodology exposed in the last two sections we have analysed the microseismic activity of the Rhine graben and surrounding regions using the focal mechanisms (Tables 1 and 2) published by

Ahorner *et al.* (1983), Bonjer *et al.* (1984) and Pavoni (1987).

Northern Switzerland and Jura Mountains. Superimposition of the right dihedra of 16 focal mechanisms (Table 1) from the Helvetic Alps, the northern Switzerland plateau and the Jura Mountains clearly defines common compressional and tensional horizontal zones orientated NNW–SSE and WSW–ENE, respectively (indicating that a unique stress deviator may be computed). Inversion of data gives a stress deviator whose σ_1 and σ_3 axes trend N158.5° ± 5° and N68.5° ± 3°, respectively (Fig. 3b and Table 3 PLS). This is in agreement with Pavoni's (1987) previous assumptions. The σ_2 axis is vertical indicating a strike-slip regime.

The southern part of the Rhine graben. Superimposition of the right dihedra of 14 normal (Table 1) and nine

Table 1. Extensional focal solutions used to compute the mean states of stress in the Rhine graben and surrounding regions. Region and Date give the location and date of earthquakes. References (Ref.): 1, Ahorner *et al.* (1983); 2, Bonjer *et al.* (1983); 3, Pavoni (1987); numbers in parentheses following the references give the original numbers of the earthquakes in these references. Planes 1 and 2 are the nodal planes

No.	Region	Ref.	Date	Plane 1 Strike (°)	Plane 1 Dip (°)	Plane 2 Strike (°)	Plane 2 Dip (°)	*T*-axis Azimuth (°)	*T*-axis Plunge (°)
	FIC1 Rhenish Massif								
1	Roermond	1(01)	5/06/80	134	72NE	64	45SE	12	18NE
2	Waldfeucht	1(02)	22/05/82	212	52SW	169	49NE	54	01NE
3	Brauweiler	1(03)	06/11/77	17	48NW	34	42SE	296	03NW
4	Euskirchen	1(05)	29/03/78	122	42SW	132	48NE	39	04NE
5	Sinzig	1(06)	30/04/78	163	65SW	163	25NE	252	20SW
6	Marienberg	1(07)	28/06/82	83	58SE	152	60NE	28	01NE
7	Ochtendung	1(08)	77–81	124	60NE	109	30SW	28	15NE
8	Braubach	1(09)	78–81	130	60NE	75	45SE	20	08NE
9	St Goar	2(01)	31/12/80	113	64SW	170	42NE	227	13SW
	FIC2 Northern part of the Rhine graben								
10	Idstein	2(02)	7/03/77	062	42NW	118	60SW	185	08SW
11	Weisbaden	2(04)	4/11/79	140	34NE	153	56SW	237	12SW
12	Darmstadt	2(06)	7/06/79	100	42NE	145	58SW	215	10SW
13	Undenheim	2(07)	11/02/81	044	80NW	060	10SE	318	35NW
14	Oppenheim	2(08)	31/07/79	002	85NE	094	75NE	228	14SW
15	Lorsh	2(09)	09/04/77	105	50NE	153	49SW	41	01NE
16	Grossachsen	2(10)	12/07/71	181	52NE	142	45SW	73	05NE
17	Speyer	2(11)	28/02/72	201	65NE	195	25NW	108	21SE
18	Hanau	1(13)	21/09/81	13	80SE	112	50SW	68	20NE
19	Schwetzingen	1(18)	3/04/79	155	30NE	162	60SW	248	18SW
	FIC3 Southern part of the Rhine graben								
20	Enklosterle	2(14)	12/10/80	100	60SW	177	70NE	234	03SW
21	Dornstetten	2(15)	23/11/79	160	50SW	305	45NE	233	03NW
22	Mohlsheim	2(16)	16/12/77	30	50SE	198	35NW	115	10SE
23	Wyhl	2(18)	26/07/76	190	70NW	296	54NE	246	10SW
24	Epinal	2(20)	12/11/74	20	80SE	119	70SW	69	07NE
25	Albstadt	2(22)	3/09/78	20	75NW	113	77NE	66	02NE
26	Wolterdingen	2(23)	29/02/76	12	60SE	133	50SW	77	06NE
27	Heitersheim	2(25)	5/03/75	145	40SW	330	50NE	59	05NE
28	Kaizerstuhl	2(27)	30/04/78	4	80NW	105	45NE	252	22SW
29	Bantzenheim	2(28)	7/11/75	90	70S	170	60NE	218	08SW
30	Sierentz	3(17)	28/01/80	105	75S	12	80E	60	04E
31	Sierentz	3(19)	5/09/80	102	76S	10	82E	58	04E
32	Sierentz	3(20)	23/03/81	147	22S	43	84E	115	36S
33	Schopfheim	3(25)	4/10/82	27	70E	124	71S	256	1W
	PLS Northern Switzerland–Jura Mountains								
34	Langenthal	3(05)	26/04/74	44	40E	290	70N	240	51W
35	Bodensee	3(09)	26/03/76	123	90	213	90	76	00
36	St. Blaise	3(08)	22/03/73	193	90	103	90	58	00
37	Bodensee	3(07)	2/03/76	121	90	211	90	76	00
38	Horgen	3(10)	21/11/77	124	85S	33	80E	259	04W
39	Oensingen	3(12)	13/08/78	120	67S	26	80E	76	08E
40	Baretswill	3(13)	28/08/78	9	40E	137	62S	249	12W
41	Murten	3(15)	3/07/79	284	86N	14	88E	240	04W
42	Albis	3(16)	30/11/79	205	86W	295	89N	70	02E
43	Wetzikon	3(27)	11/01/84	211	89W	121	89S	76	01E
44	SudAlbis	3(28)	5/09/84	358	56N	112	59S	235	02W
45	Sarnen	3(02)	14/03/64	189	51W	81	70E	37	44E
46	Glarus	3(03)	29/09/71	203	86W	113	86S	68	06E
47	Murgtal	3(06)	29/12/75	87	80E	355	80N	41	01E
48	Valderuz	3(11)	7/04/78	265	76W	172	79S	219	02W
49	Hauenstein	3(22)	5/09/82	97	70S	5	85E	53	10E

Table 2. Compressional focal mechanisms in the Rhine graben and surrounding regions. Same symbols as in Table 1

No.	Region	Ref.	Date	Plane 1 Strike (°)	Plane 1 Dip (°)	Plane 2 Strike (°)	Plane 2 Dip (°)	T-axis Azimuth (°)	T-axis Plunge (°)
	FIC2 (i) Northern part of the Rhine graben								
50	Echzell	2(03)	4/11/75	063	80NE	162	50NE	195	34SW
51	Geroldstein	2(05)	8/05/77	045	45NW	045	45SE	000	90
	FIC3 (i) Southern part of the Rhine graben								
52	Rhinau	2(17)	27/10/79	012	90	102	80SW	057	08NE
53	Schlusht	2(19)	18/08/81	037	65NW	117	70SW	077	34NE
54	Waldkirch	2(21)	27/01/79	060	82SE	163	60SW	012	26NE
55	Schopfheim	2(26)	15/08/77	022	80SE	120	40NE	255	30SW
56	Delle	2(29)	11/02/78	128	60SW	062	54NW	092	50SE
57	Langenthal	2(31)	26/04/74	110	65NE	045	35SE	240	51SW
58	Dinkelberg	2(32)	21/05/74	042	72SE	115	41NE	275	44W
59	Epinal	1(20)	03/03/81	109	71SW	026	70NW	067	08NE
60	Sierentz	1(27)	15/07/80	040	90	130	80SE	086	08E

Table 3. Parameters of the deviatoric stress tensor derived from the focal mechanisms of the Rhine graben and surrounding regions

Name region	σ_1 Strike (°), Dip (°)	σ_2 Strike (°), Dip (°)	σ_3 Strike (°), Dip (°)	R value
PLS	158 ± 5, 3 ± 4	210, 86	68.5 ± 3, 3 ± 5	0.393 ± 0.11, −0.24
PLS (inversion)	339 ± 2, 5 ± 2.4	186 ± 18, 85 ± 2	69 ± 2, 2 ± 1.2	0.36 ± 0.02
FIC3	144, 85	313.7 ± 5, 2 ± 2	43.6 ± 5, 5 ± 2	0.462 ± 0.2
FIC3 (inversion)	174 ± 18, 81 ± 3	319 ± 3, 7 ± 3	50 ± 4, 5 ± 2	0.40 ± 0.02
FIC2	161, 81	310 ± 5, 8 ± 3	40.6 ± 5, 5 ± 3	0.583 ± 0.2
FIC2 (inversion)	179 ± 16, 80 ± 2	310 ± 2, 6 ± 2	40 ± 2, 7 ± 2	0.42 ± 0.1
FIC1	154, 73	314 ± 5, 16.5 ± 5	46 ± 5, 5.3 ± 4	0.288 − 0.1, +0.2
FIC1 (inversion)	355 ± 17, 82 ± 2	135 ± 2.5, 6 ± 2	225.5 ± 2, 5 ± 2	0.30 ± 0.05
FIC2 + 3 Normal	107.3 ± 86	313.6, 3.57	223.54, 1.76	0.49
FIC2 + 3 Reverse	316.14, 0.05	46.15, 10.74	225.8, 79.25	0.7

PLS: Northern Switzerland and Jura Mountains; FIC3 and FIC2: southern and northern parts of the Rhine graben, respectively; FIC1: Rhenish Massif; FIC2 + 3 give the solutions for the set collecting the FIC1 and FIC3 data (see Fig. 3a1 and a2). The σ_3, σ_2 and σ_1 give the azimuths (first numbers) and dips (second numbers) in degrees of the stress axes with the computed uncertainties. The stress ratio R equals $(\sigma'_2 - \sigma'_1)/(\sigma'_3 - \sigma'_1)$. Two solutions are given for each region: the first one uses a least-square method (Carey-Gailhardis & Mercier 1987), the second one a generalized non-linear inversion method (Carey-Gailhardis & Sotin 1991).

reverse (Table 2) focal mechanisms clearly shows that all the seismic fault motions cannot be modelled by a single deviator. Therefore no single stress deviator having a vertical σ_2 axis as proposed by Larroque *et al.* (1987) can model both these focal solutions. The better non-reducible solution obtained both by a method of trial and error and a generalized inversion method separates the nine reverse from the 14 normal fault plane solutions. Superimposition of the right dihedra of the normal focal mechanisms clearly defined an horizontal common extensional zone orientated NE–SW and a vertical common compressional zone. Inversion of the data gives a stress deviator whose σ_2 and σ_3 axes trend N313.7° ± 5° and N43.6 ± 5°, respectively; the vertical axis is σ_1(Fig. 4c and Table 3, FIC3).

The northern part of the Rhine graben. The same methods separate the two reverse (Table 2) from the 10 normal (Table 1) fault plane solutions. Inversion of these latter gives a deviator whose σ_2 and σ_3 axes trend N310° ± 5° and N40.6° ± 5°, respectively; the σ_1 axis is vertical (Fig. 4b and Table 3, FIC2). This agrees with the Larroque *et al.* (1987) results.

A similar solution is obtained from collating the focal mechanisms of the southern and northern parts of the Rhine graben. Clearly, the necessary condition to compute a single stress deviator is not satisfied. The above methods separate the 11 reverse from the 24 normal fault plane solutions. The former set leads to the computation of a stress deviator whose σ_2 and σ_3 axes are horizontal and trend N314° and N223.5°, respectively; the σ_1 axis is vertical (Fig. 3a1). The latter set leads to the computation of a stress deviator whose σ_1 and σ_2 axes are horizontal and trend N316° and N46°, respectively; the σ_3 axis is vertical (Fig. 3a2). As already observed for computation of states of stress from focal mechanisms of microearthquakes (see the third section of this paper and Fig. 1), these deviators are co-axial: one is the mean state of stress (TM), the other (TC) models the local reverse fault motions. As numerous geological and geophysical data show that the tectonic regime in the Rhine graben is not compressional (σ_3 vertical), it is concluded that the compressional fault motions (TC) result from kinematics instabilities, i.e from local adjustments of blocks and that the tectonic regime (TM) in the whole Rhine graben is extensional (σ_1 vertical).

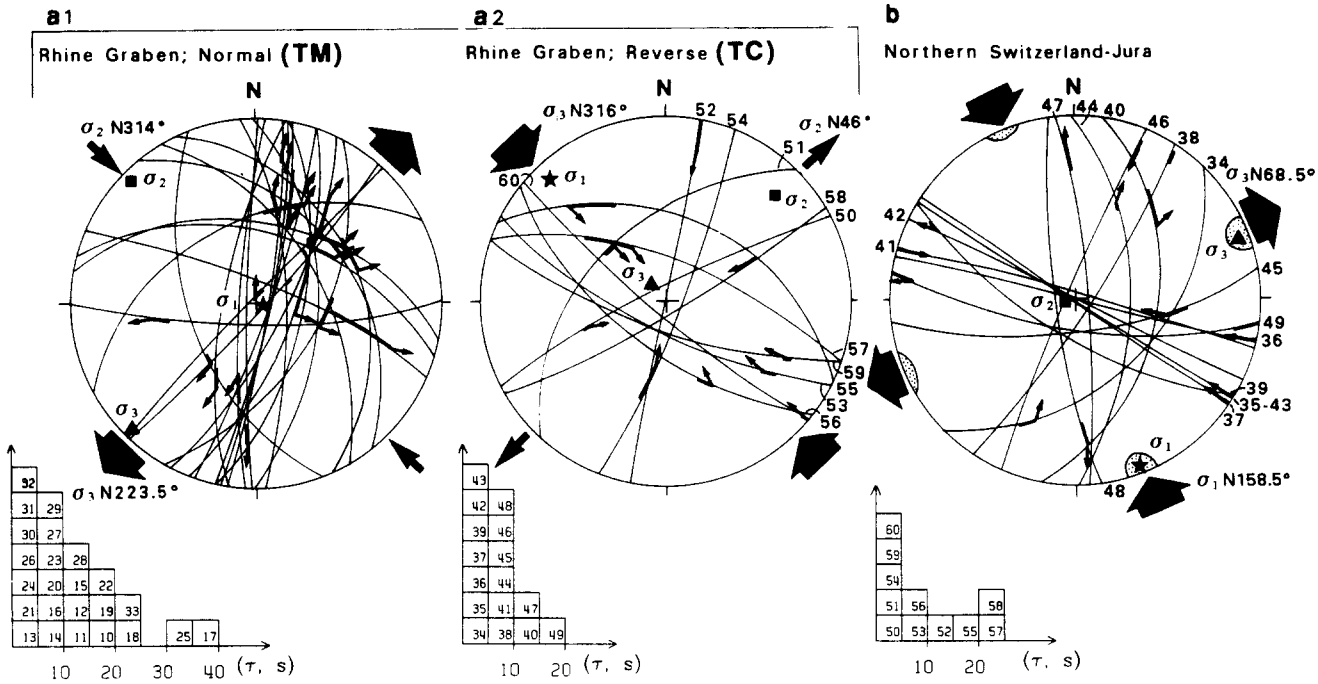

Fig. 3. Preferred seismic fault planes used to compute (a) the mean regional state of stress (a1) and the deviator (TC) which models the local compressional fault motions (a2) in the Rhine graben. (b) The mean regional state of stress in northern Switzerland. Numbers outside the stereonets refer to the numbers of the events in Tables 1 and 2. Same symbols as on Fig. 1.

The Rhenish Massif. Two reverse fault plane solutions must be also separated from the nine normal ones (Table 1). Inversion of these latter gives a deviator whose σ_2 and σ_3 axes trend N314° ± 5°, respectively (Fig. 4a and Table 3, FIC1). The σ_1 axis is vertical, and the tectonic regime is extensional.

The regional state of stress in the Rhine graben and surrounding regions and the fault motions

The seismic fault motions in the Rhine graben appear to have resulted from an extensional tectonic regime. This graben cannot be considered as a left-lateral shear zone in which left-lateral strike-slip faults are the equivalents of *R*-Riedel shears formed in an isotropic material as a result of a strike-slip faulting tectonic regime (σ_2 vertical). In the southern part of the graben, the existing faults having a mean N20°E strike (N10° to N30°) are reactivated with a predominant strike-slip component. In the northern part of the graben, the existing faults striking NW–SE, ENE–WSW or WNW–ESE are reactivated with a predominant normal component. The NE–SW orientation of the tensional σ_3 direction with respect to the orientation of existing faults explains the different observed fault motions (Fig. 4). Outside the graben, focal mechanisms are not sufficiently numerous to constrain the solutions. The Albstadt earthquake (No.25 in Fig. 2, Table 1) might result either from an extensional or a strike-slip regime. But, if the N20°-striking nodal plane is the seismic fault plane, as suggested by Bonjer *et al.* (1984), then its motion agrees with the extensional regime of the southern part of the graben.

The computed σ_2 axes which are the $\sigma_{H\ max}$ axes trend N313.7°, N310° and N314° in the Rhine graben and in the Rhenish Massif (Fig. 4). They are surprisingly similar in orientation on such a large area, suggesting that these normal fault plane solutions of microearthquakes are statistically representative of the regional state of stress. They are in agreement with the mean $\sigma_{H\ max}$ direction deduced from *in situ* stress measurements (Fig. 5). In northern Switzerland $\sigma_{H\ max}$ trends N158.5° (Fig. 3b). This result appears to be in good agreement with the NNW–SSE direction of the $\sigma_{H\ max}$ previously proposed (Pavoni 1987, Deichmann 1990). Thus, the $\sigma_{H\ max}$ direction shows as approximately 25° anticlockwise rotation from northern Switzerland toward the north. This change of direction (Bonjer *et al.* 1984) is clear from the northern border of the Jura Mountains or the southernmost part of the Rhine graben. This supports the idea that stresses generated by the Alps system are superimposed on a stress field at the European plate scale whose $\sigma_{H\ max}$ direction trends NW–SE in France (Baumann & Illies 1983).

The $\sigma_{H\ max}$ value increases from the Rhine graben region towards the Alps as shown by *in situ* stress measurements (Baumann & Illies 1983) and by the analysis of the focal mechanisms of microearthquakes (Fig. 5). This agrees with the idea that the active extension in the Rhine graben and Rhenish Massif is possibly due to a 'blob' effect (McKenzie 1978, Fleitout & Froidevaux 1982). A dense mantle sinking in the asthenosphere below the Alps (Fig. 6) would increase the horizontal compression near the Alps and create extension at its periphery. This stress field is very different from those observed in the high mountains of the Andes and Himalayas, Tibet, where the value of the vertical σ_{zz} axis increases with topography and crustal thickness, and may exceed $\sigma_{H\ max}$ to become σ_1, thus allowing extension to occur in the high plateau regions.

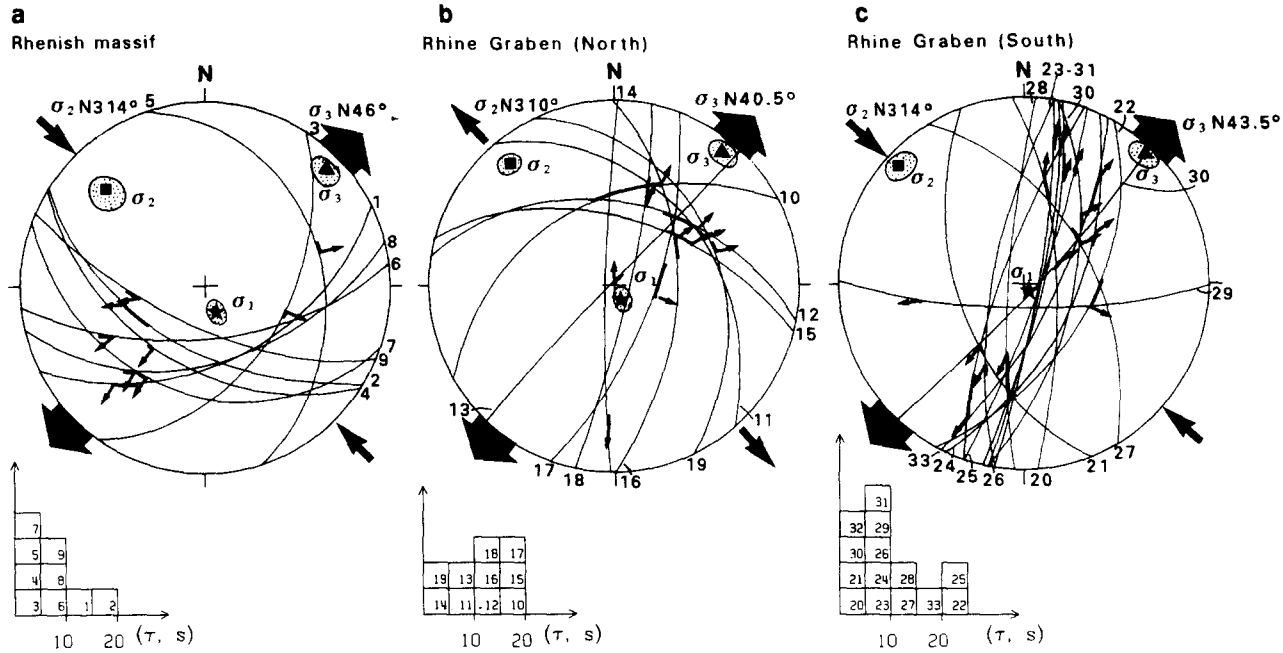

Fig. 4. Preferred seismic fault planes used to compute the mean regional state of stress in (a) the Rhenish Massif and (b & c) the Rhine graben. Numbers outside the stereonets refer to the numbers of the events in Table 1. Same symbols as on Fig. 1.

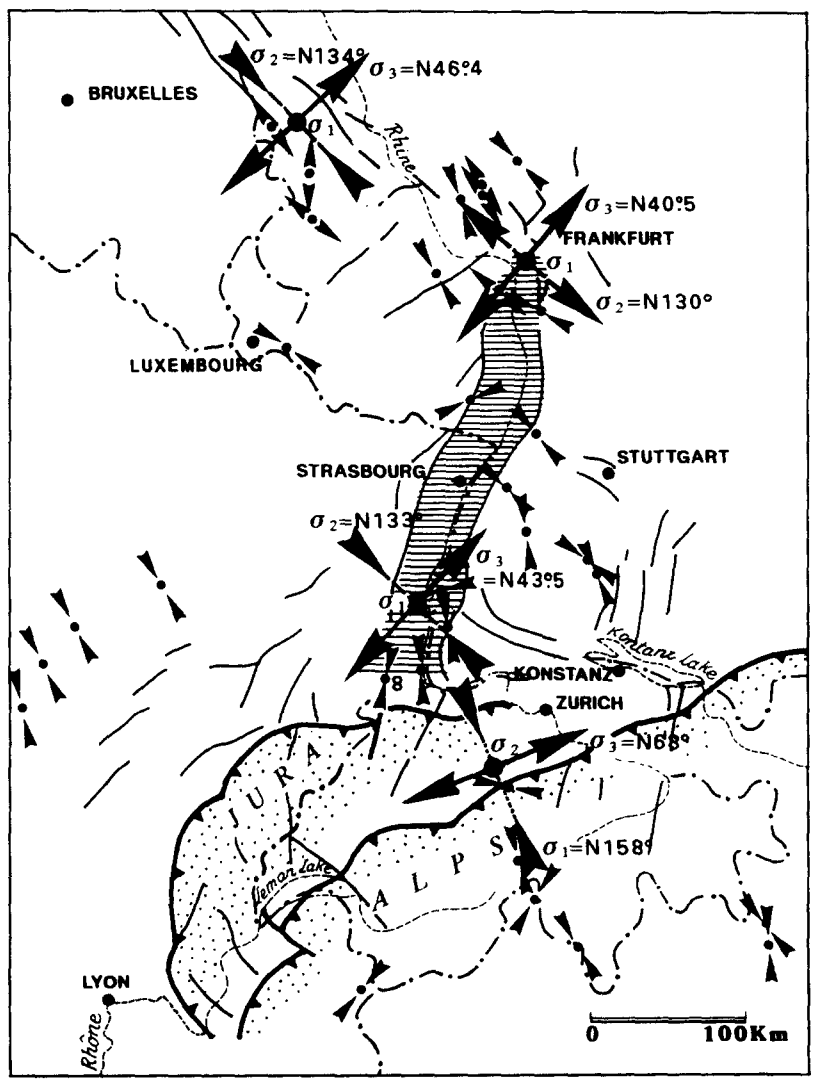

Fig. 5. Horizontal principal stress directions of the mean state of stress (TM) in the Rhine graben and surrounding regions deduced from the inversion of the focal mechanisms of earthquakes (large arrows). Directions of $\sigma_{H\,max}$ deduced from *in situ* measurements (Baumann & Illies 1983) are added (small arrow heads).

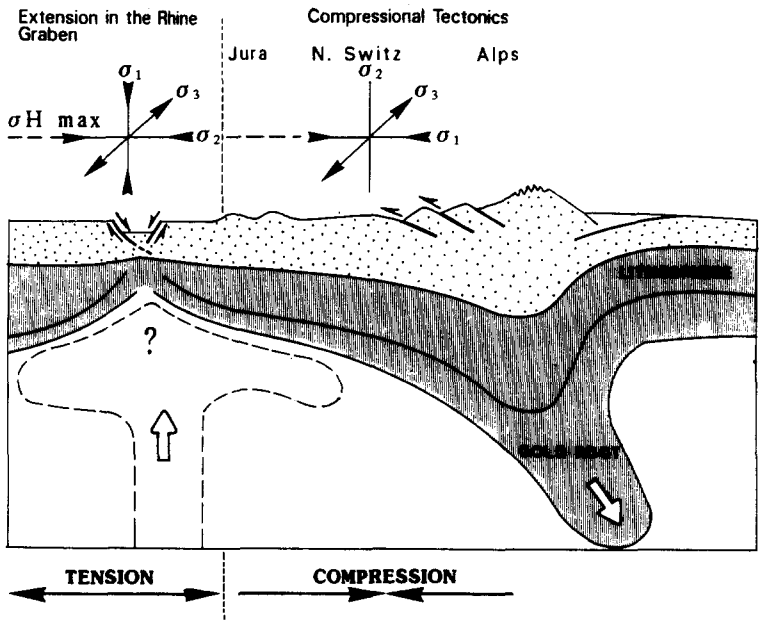

Fig. 6. Schematic diagram suggesting tension in the Alpine foreland and compression in the Alps as a result of a cold lithosphere sinking in the mantle (after Fleitout 1984). The states of stress represented above the sketch are those deduced from the inversion of the focal mechanisms (Fig. 5).

CONCLUDING REMARKS

Analysis of focal mechanisms of microearthquakes shows that, as a result of incompatibilities of block motions in an assemblage of rigid or elastic blocks, deformation of a fractured body of rock in general is heterogeneous. Thus, such focal mechanism sets cannot be modelled by a single stress deviator. Analyses of several examples show that they are composed of a main group whose fault motions result from a mean state of stress (TM) in good agreement with the regional tectonic regime; the remaining complex fault motions are explained by a compressional (TC) and/or a tensional deviator (TE). An important observation is that, within the computed uncertainties of the stress directions, these latter deviators are co-axial with the mean state of stress (TM). These deviators (TC, TE) statistically model the local fault-slips due to the incompatabilities of block motions and cannot be considered as other states of stress. Therefore the 'permutation of the stress values' of these co-axial stress tensors are not indicative of real permutations of the principal stress axes corresponding to temporal changes in the regional state of stress in response to changes in the magnitude of the boundary or of the body forces, as those observed for example in the Andes and in Tibet (see Mercier *et al.* 1991).

It therefore follows that even if the regional state of stress is known, the movement on a minor fault plane of known strike and dip, cannot be surely predicted. Several motions (TC, TE) different from that predicted by the mean state of stress (TM) may exist; these TC and TE motions are kinematic instabilities. As a consequence all the motions shown by striated faults or by focal mechanisms are not necessarily significant of the regional tectonic regime. This is well illustrated by the microseismic activity of the Rhine graben. The compressional fault motions are kinematic instabilities (i.e local fault motions). The extensional fault motions indicate a tensional state of stress (σ_1 vertical) with N45°-trending σ_3 axis which is statistically significant of the regional tectonic regime.

Thus to model the kinematics of faults in a fractured body of rocks, we suppose (Mercier *et al.* 1991) the same basic hypotheses as those proposed by Carey & Brunier (1974): (1) homogeneity and isotropy of the material, (2) small fault displacements, no ductile deformation, no rotations of the fault planes (see the second section of this paper). But the computation assumes the following different hypotheses. (3) The brittle deformation resulting from a tectonic event is heterogeneous and is modelled by several deviators. One of them is the mean state of stress acting in the body of rock; the others are co-axial with the previous one and account for the local fault motions due to adjustments of blocks. (4) The slip responsible for the striation occurs on each fault plane in the direction and sense of the shear stress resolved on the fault plane due to one of these deviators. (5) The slips on the fault planes are not independent as a result of incompatibilities of block motions in the body of rocks.

The simple mechanical model of homogeneous state of stress and independent fault motions used to interpret fault kinematics in terms of stress (Carey & Brunier 1974) is therefore valid only if there are no incompatibilities of block motions. Indeed when studying fault kinematics from field data, computation often leads to a homogeneous state of stress. It is noteworthy that striations measured in the field are often growth fibers and stylolitic striations which result from creep faulting. In this case if a pressure-solution–crystallization process is active, it may accommodate the incompatibilities of block motions. Kinematics of large seismic faults shown

by focal mechanisms from teleseismic records may often lead to the computation of a single stress deviator. Probably in this case, the incompatibilities of block motions are accommodated by internal cataclastic deformation of the the large blocks separated by the major faults. Thus the kinematics of minor faults probably reflect the internal deformation of large blocks rather than the regional state of stress. Therefore, when studying fault kinematics in terms of stress, only the coherence of the results shown by a statistical analysis of the data obtained at numerous sites is a convincing argument for a reliable information on the regional state of stress.

Acknowledgements—This work has been supported by the programme DBT 'Instabilités' (contribution CNRS-INSU-DBT No.390), Institut National des Sciences de l'Univers. We thank A. Etchecopar and J. Angelier for their helpful critical reviews.

REFERENCES

Ahorner, L., Baier, B. & Bonjer, K. P. 1983. General pattern of seismotectonic dislocations and the earthquake-generating stress field in Central Europe between the Alps and the North Sea. In: *Plateau Uplift* (edited by Fuchs, K. *et al.*). Springer, Berlin, 187–197.

Angelier, J. & Goguel, J. 1979. Sur une méthode simple de détermination des axes principaux des contraintes pour une population de failles. *C. r. Acad. Sci.,Paris* **D288**, 307–310.

Armijo, R. & Cisternas, A. 1978. Un problème inverse en microtectonique cassante. *C. r. Acad. Sci., Paris* **D287**, 595–598.

Baumann, H. & Illies, H. J. 1983. Stress field and strain release in the Rhenish Massif. In: *Plateau Uplift* (edited by Fuchs, K. *et al.*) Springer, Berlin, 177–186.

Bergerat, F. 1985. Déformations cassantes et champs de contrainte tertiaires dans la plateforme européenne. Unpublished thèse d'Etat, Université P. & M. Curie, Paris.

Bonjer, K.-P., Gelbke, C., Gilg, B., Rouland, D., Mayer-Rosa, D. & Massinon B. 1984. Seismicity and dynamics of the Upper Rhine graben. *J. geophys.* **55**, 1–12.

Bott, M. H. P. 1959. The mechanics of oblique slip faulting. *Geol. Mag.* **96**, 109–117.

Cabrera, J., Sébrier, M. & Mercier, J. L. 1991. Plio-Quaternary geodynamic evolution of a segment of the Andean Peruvian Cordillera located above the change in the subduction geometry: The Cuzco region. *Tectonophysics* **190**, 331–362.

Carey, E. 1979. Recherche des directions principales de contraintes associées au jeu d'une population de failes, *Rev. geol. dyn. Géogr. phys.* **21**, 57–66.

Carey, E. & Brunier, B. 1974. Analyse théorique et numérique d'un modèle mécanique élémentaire appliqué à l'étude d'une population de failes. *C.r.Acad Sci., Paris* **D279**, 891–894.

Carey-Gailhardis, E. & Mercier, J. L. 1987. A numerical method for determining the state of stress using focal mechanisms of earthquake populations: application to Tibetan teleseisms and microseismicity of southern Peru. *Earth Planet. Sci. Lett.* **82**, 165–179.

Carey-Gailhardis, E. & Sotin, C. 1991. Application of the generalized nonlinear inversion theory to the determination of fault planes and principal stress directions from analysis of focal mechanisms. In: *Failles, analyse et modélisation, Réunion spéciale Soc. géol. Fr. Abs.* Paris, 18.

Cornet, F. H. & Burlet, D. In press. Eight regional stress determinations in France by hydraulic tests in borehole. *J. geophys. Res.*

Deichmann, N. 1990. Seismizität der Nordschweiz 1987–1989, und Auswertung der Erdbebenserien von Günsberg, Läufelfingen und Zeglingen Schweizericher Erdbebendienst, *Technischer Bericht* **90-46**.

Deschamps, A. & King, G. C. P. 1984. The Campania Lucania (southern Italy) earthquake of 23 November 1980. *Earth Planet. Sci. Lett.* **62**, 296–304.

Etchecopar, A., Vasseur, G. & Daignères M. 1981. An inverse problem in microtectonics for determination of stress tensors from fault striation analysis. *J. Struct. Geol.* **3**, 51–65.

Fleitout, L. 1984. Thermomechanical models of lithospheric deformation; application to the tectonics of Western Europe. Unpublished Thèse d'Etat, University of Paris-Sud.

Fleitout, L. & Froidevaux, C. 1982. Tectonics and topography for a lithosphere containing density heterogeneities. *Tectonics* **1**, 21–56.

Gephart, J. W. & Forsyth, D. W. 1984. An improved method for determining the regional stress tensor using earthquake focal mechanism data: application to the San Fernando earthquake sequence, *J. geophys. Res.* **89**, 9305–9320.

Hatzfeld, D., Christodolou, A. A, Scordilis, E. M., Panagiotopoulos, D. & Hatzidimitriou, P. M. 1987. A microearthquake study of the Mygdonian graben (northern Greece). *Earth Planet. Sci. Lett.* **81**, 379–396.

Jackson, J. & McKenzie, D. 1983. The geometrical evolution of normal fault systems. *J. Struct. Geol.* **5**, 471–482.

Julien, Ph. & Cornet, F. H. 1987. Stress determination from aftershocks of the Campania–Lucania earthquake of November 23, 1980. *Annls Geophys.* **5B**, 289–300.

Larroque, J. M. Etchecopar, A. & Philip H. 1987. Evidence for the permutation of stresses σ_1 and σ_2 in the Alpine foreland: the example of the Rhine graben. *Tectonophysics* **144**, 315–322.

McKenzie, D. P. 1969. The relations between fault plane solutions for earthquakes and the directions of the principal stresses. *Bull. seism. Soc. Am.* **59**, 591–601.

McKenzie, D. P. 1978. Active tectonics of the Alpine-Himalayan belt: the Aegean Sea and surrounding regions. *Geophys. J. R. astr. Soc.* **55**, 217–254.

Mattauer, M., Laurent, P. & Petit, J. P. 1991. Space and time variations in the Pyrenean stress field: a case study of a Languedoc outcrop. In: *Mechanical Instabilities in Rocks and Tectonics. Terra Abs.* (Suppl. 5 to *Terra Nova* **3**, 26).

Mercier, J. L. & Carey-Gailhardis, E. 1989. Regional state of stress and characteristic fault kinematics instabilities shown by aftershock sequences: the aftershock sequences of the 1978 Thessaloniki (Greece) and 1980 Campania-Lucania (Italia) earthquakes as examples. *Earth Planet. Sci. Lett.* **92**, 247–264.

Mercier, J. L., Carey-Gailhardis, E. & Sébrier, M. 1991. Paleostress determinations from fault kinematics: application to the neotectonics of the Himalayas–Tibet and the Central Andes. In: *Tectonic Stress in the Lithosphere* (edited by Whitmarsh, R. B., Bott, M. H. P., Fairhead, J. D. & Kusznir, N.). *Phil Trans. R. Soc. Lond.* **A337**, 41–52.

Pavoni, N. 1987. Seismotektonik der Nordschweiz, *Eclog. geol. Helv.* **80**, 461–472.

Pollard, D. D. & Saltzer, S. D. 1991. Stress inversion methods: are they based on faulty assumptions. In: *Mechanical Instabilities in Rocks and Tectonics. Terra Abs.* (Suppl. 5 to *Terra Nova* **3**, 31).

Rivera, L. A. & Cisternas, A. 1987. Stress tensor and fault plane solutions for a population of earthquakes. (Abs.) *Terra Cognita* **7**, 461.

Rummel, F. & Hansen, J. 1988. Stress measurements in HDR research, Workshop RCS, Strasbourg, 6–7 December.

Segall, P. & Pollard, D. D. 1980. Mechanisms of discontinuous faults. *J. geophys. Res.* **85**, 4350–4387.

Vasseur, G., Etchecopar, A. & Philip, H. 1983. Stress state inferred from multiple focal mechanisms. *Annls Geophys.* **1**, 291–298.

Villemin, T. & Bergerat, F. 1985. Tectonique cassante et paléocontraintes tertiaires de la bordure du Fossé Rhénan (R.F.A). *Oberrhein. geol. Abh.* **34**, 63–87.